



Experimental study on the pressure drop of helium purge gas in particle crushing pebble beds

Hao Cheng^a, Zheng Fang^{a,b}, Bing Zhou^{a,*}, Baoping Gong^a, Shanshan Bu^{b,*}, Zhenzhong Li^b, Deqi Chen^b

^a Southwestern Institute of Physics, Chengdu, 610225, China

^b Key Laboratory of Low-Grade Energy Utilization Technologies & System, Chongqing University, Chongqing, 400044, China

ARTICLE INFO

Keywords:

Pressure drops

Pebble bed

Helium

Flow characteristics

Breakage rate

ABSTRACT

The solid breeder blanket is a critical component in fusion reactor, where helium purge gas flows through the solid breeder pebble bed to carry out the tritium generated during the fusion process. The flow pressure drop of helium purge gas within the breeder pebble bed is a significant parameter affecting the design of the tritium extraction system. Previous studies have indicated that the helium flow in the breeder pebble bed conforms to the theory of porous media flow. However, due to potential pebble breakage during the plasma operation, the pressure drop characteristics of the helium flow in breeder pebble bed may change as the void structure changes. The objective of this study is to measure the variation in flow pressure drop of the breeder pebble bed under different pebble crushing conditions. The flow pressure drops of intact beds (Alumina, diameter 1–1.2 mm) and four groups with different pebble breakage rates (3%, 5%, 7%, 9%) are measured using the pebble bed pressure drop test facility. The following results are obtained through experimental research: (1) The Ergun equation, Fomenko equation, and Reichelt equation can all reasonably match the experimental results of intact pebble beds; (2) The pressure drop across the pebble bed increases with the increase in pebble breakage rate, reaching approximately 1.6 times that of the intact bed at a 9% breakage rate; (3) A correlation for predicting the pressure drop of the broken pebble bed is established by introducing the pebble breakage rate (η) into the Ergun equation, which can be used to determine the pressure drop variation within a conservative range of breakage rates.

1. Introduction

The pebble bed in fusion breeding blanket is a crucial component in fusion reactor for tritium breeding. Among various design concepts, the helium-cooled solid breeder is one of the most prominent designs in breeding blankets. The solid breeder is comprised of lithium ceramic breeder pebble materials such as lithium metasilicate (Li_4SiO_4) and lithium titanate (Li_2TiO_3), filled in a pebble bed configuration around the vacuum vessel to absorb high-energy neutrons generated by fusion reaction, the lithium in the breeder will react with the neutrons to release heat and tritium, then the low-pressure helium purge gas is used to carry out the tritium. In the Test Blanket Module (TBM) programs of the ITER project [1], the Helium-Cooled Ceramic Breeder (HCCB) proposed by China and the Helium-Cooled Pebble Bed (HCPB) proposed by EU are both considered the Li_4SiO_4 pebbles with 1 mm diameter as tritium breeder, and helium gas as the purge gas. In China Fusion Engineering Test Reactor (CFETR) tritium breeding blanket design concept

[2], the HCCB is also a competitive option.

The pressure drop of the helium purge gas in the blanket is an important design parameter for the tritium extraction system (TES). To meet the design requirements of the breeding blanket, researchers have studied the flow characteristics of helium in the breeder bed. Abou-sena et al. [3,4] conducted pebble bed pressure drop experiments using glass pebbles and Li_4SiO_4 pebbles with different size distributions (0.25–1.2 mm), the test section is a cylindrical container with a diameter of 30 mm and a length of 100 mm, with flow velocities ranging from 0.5 m/s to 4 m/s, the experimental results exhibited good agreement with the Ergun equation. Wang et al. [5] performed pebble bed flow pressure drop experiments in rectangular channels (20 × 20 mm) to match the design characteristics of the CFETR. The pebble beds were filled with high-precision stainless steel balls with particle sizes ranging from 0.8 mm to 2.0 mm. They determined suitable constants of the Ergun equation based on pressure drop data from different particle sizes. Liu et al. [6] investigated the pressure drop characteristics of helium flow in

* Corresponding authors.

E-mail addresses: zhoub@swip.ac.cn (B. Zhou), shanshanbu@cqu.edu.cn (S. Bu).

<https://doi.org/10.1016/j.fusengdes.2024.114631>

Received 13 May 2024; Received in revised form 28 July 2024; Accepted 12 August 2024

0920-3796/© 2024 Elsevier B.V. All rights are reserved, including those for text and data mining, AI training, and similar technologies.

rectangular channel pebble beds under Darcy and Forchheimer flow regime. Panchal et al. [7] studied the nitrogen flow pressure drop of stainless steel balls (1 mm, 2 mm, 3 mm, 4 mm), Al_2O_3 balls (1 mm, 1.5 mm), and Li_2TiO_3 balls (1 mm, 1.3 mm) in circular channel pebble beds. All the above studies are based on unitary pebble beds. However, in some breeder design concepts, ceramic breeder particles are mixed with neutron multipliers, forming a binary pebble bed. Recently, research by Liu et al. [8] investigated the flow pressure drop of helium in both unitary and binary breeder pebble beds. By fitting the viscous and inertial terms based on the Ergun equation with experimental data, they found that the pressure drop in binary pebble beds is influenced by the diameter ratio of the binary particles and the volume fraction of the larger particles.

The studies primarily focused on the flow pressure drop of intact blanket pebble beds. However, during plasma operation, ceramic breeder particles are subjected not only to neutron irradiation damage from fusion but also to pressure from the surrounding structure due to differences in thermal expansion coefficients [9]. The particle crushing phenomenon has been observed in relevant experiments. Van Til et al. [10] through scanning electron microscopy, observed significant particle cracking and fragmentation of lithium silicate pebble bed particles after irradiation. Dell'Orco et al. [11] based on the ITER helium-cooled blanket simulation facility HELICHETTA, studied the strain response of Li_4SiO_4 pebble beds under cyclic thermal loads and observed pebble fragmentation after the experiment. Additionally, to study the crushing behavior of ceramic breeder particles, many experiments and numerical study based on the discrete element method (DEM) have been conducted. Zhao et al. [12] investigated the influence of plate material on the contact strength of Li_4SiO_4 pebbles in crush tests and proposed an energy-based method for predicting the critical contact force. Desu et al. [13] studied the impact of high temperatures on the crushing load of lithium titanate particles. Annabattula et al. [14] explored the influence of particle size on the crushing load. Lei et al. [15] studied the crushing behavior of individual breeder particles during compression using the finite element method with ANSYS software. Wang J et al. [16] introduced fractal theory to describe the relationship between the original particles and their fragments.

Particle crushing will change the bed packing structure, thereby influencing the flow pressure drop characteristics of the breeder pebble bed, which may introduce uncertainties in the thermal conversion and

tritium extraction functions of fusion blankets. Therefore, it is necessary to evaluate changes in flow resistance resulting from particle crushing. This experiment used the pebble bed pressure drop test facility designed and manufactured by the Southwestern Institute of Physics, conducted a series of pressure drop experiments on Al_2O_3 pebble bed. The relationship between different helium flow rates, pebble bed channel length, particle breakage rate and helium pressure drop were studied, and a correlation was established for predicting the pebble bed pressure drop under different particle breakage through experimental data.

2. Experimental setup and procedures

The experimental setup used in this study is depicted in Fig. 1. It consists of components such as a helium gas cylinder, a pressure reducing valve, an external heating jacket, the test section, and corresponding measurement devices. The experimental loop operates as an open system, where helium gas is not recycled. The high-pressure helium gas cylinder provides the driving force for helium flow in the pebble bed. Helium gas passes through the pressure reducing valve and is controlled by a digital mass flow controller (DMFC) to regulate the flow rate. The DMFC has a range of 150 SLM with an accuracy of $\pm 0.35\%$ F.S. ($<35\%$ F.S.) and $\pm 1\%$ F.S. ($>35\%$ F.S.). The helium gas flows through the pebble bed and is directly discharged into the atmosphere. A vacuum pump is installed at the end of the facility to evacuate the system before experiments and to ensure sealing performance. The helium gas used in the experiment is sourced from a cylinder with a pressure of 15 MPa and a purity of 99.999%. Fig. 2 shows the experimental facility in the Southwestern Institute of Physics.

The pebble bed test section is a long cylindrical container with a diameter of 50 mm and a length of 600 mm, as depicted in Fig. 3. Pressure guide tubes are installed along the test section at 50 mm, 150 mm, 250 mm, 350 mm, 450 mm, and 550 mm. These guide tubes are connected to the inlet of the test section, each guide tube is equipped with a valve and connected to three differential pressure transmitters (DPT) of different ranges to measure the local pressure differentials from the inlet. The ranges of the three DPT are 0.1–2 kPa, 0.5–10 kPa, and 1–100 kPa, with an accuracy level of $\leq \pm 0.04\%$. Additionally, a K-type thermocouple is installed in each guide tube to measure the temperature distribution along the centerline of the pebble bed. Absolute pressure sensors and thermocouples are installed at the inlet and the outlet of the

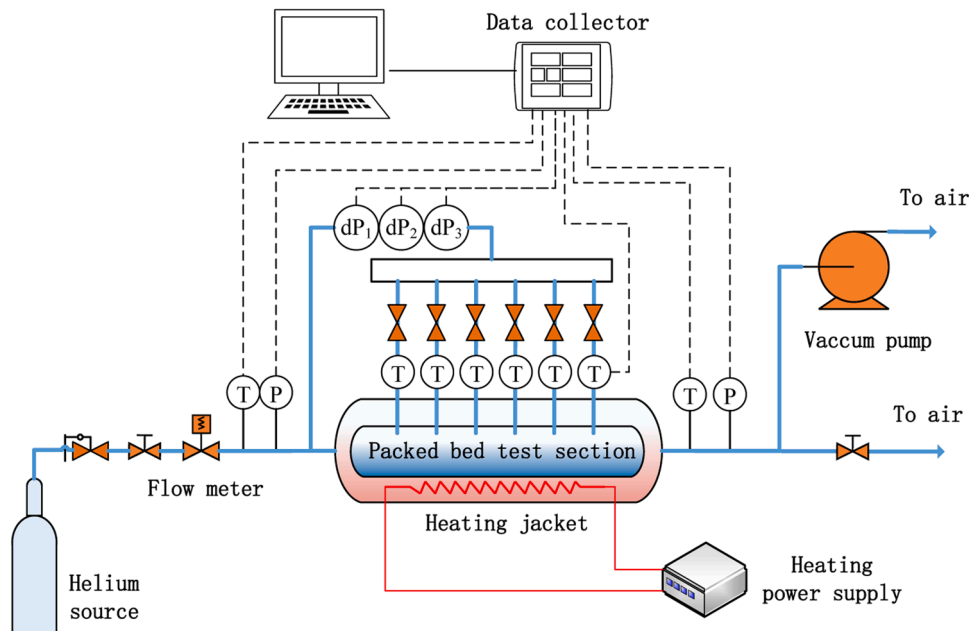


Fig. 1. Schematic diagram of the helium flow characteristics experimental facility.



Fig. 2. Diagram of the experimental facility.

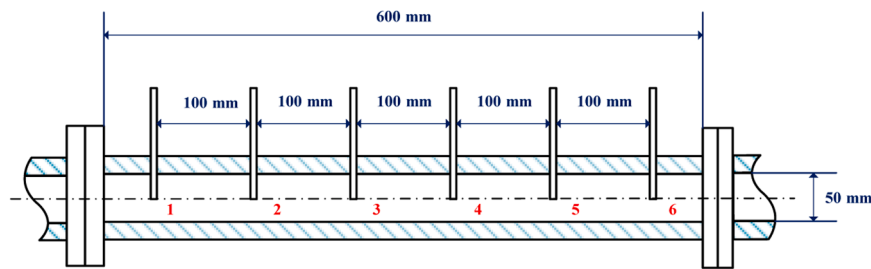


Fig. 3. Schematic diagram of the experiment test section.

test section to measure the temperature and pressure of the gas. Filters and copper piece are used at both ends of the test section to seal the pebble bed particles and helium gas, as shown in Fig. 4. The experimental setup can also conduct flow pressure drop experiments at different pebble bed temperatures by heating the test section, as illustrated in Fig. 5. An electric heating jacket is placed outside the test section, composed with insulation materials and heating resistance wires. The heating temperature can be controlled by adjusting the heating power to meet the experimental requirements for pressure drop test at different temperatures. All sensors in the experimental setup are connected to a data acquisition system.

Two types of Al_2O_3 particles were used in this experiment to simulate the breeder particles in the blanket, their parameters see Table 1. The Al_2O_3 particles with a diameter distribution of 1.0-1.2 mm were used to simulate intact Li_4SiO_4 particles in the helium-cooled solid blanket pebble bed. On the other hand, Al_2O_3 particles with a diameter distribution of 0.2-0.4 mm were employed to simulate sub-particles generated from the breakage of larger particles. A comparison between the two types of particles is illustrated in Fig. 6. In practical scenarios, the size distribution of fragmented particles resulting from particle breakage will

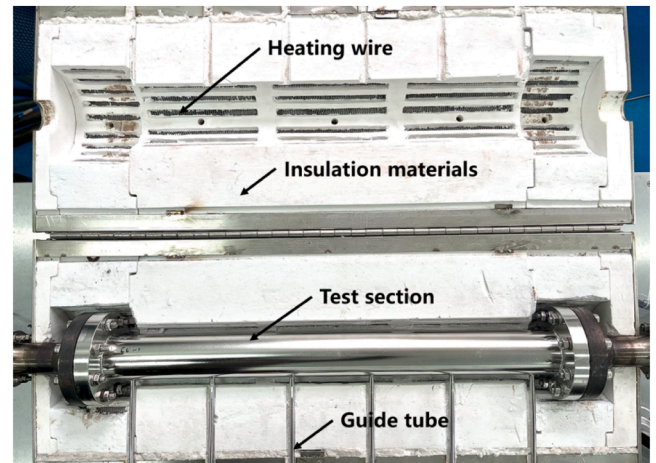


Fig. 5. The heating jacket of the test section.

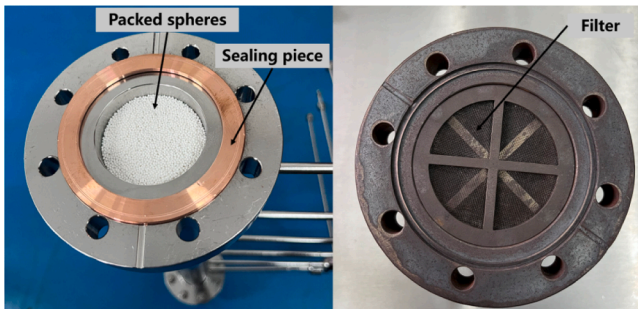


Fig. 4. Sealing of test section.

Table 1
Pebble parameter.

ID	Material	Density, g/ cm ³	Diameter range, mm	Sphericity	Average diameter, mm
A0	Al2O3	3.7	1.0-1.2	0.955	1.103
A1	Al2O3	3.7	0.2-0.4	0.853	0.301

be broader than just 0.2-0.4 mm. The selection of this narrow size range is to consider an extreme scenario of pebble bed particle crush, and smaller sub-particles may be carried out of the pebble bed region by the purge helium gas passing through the pebble bed outlet filter.

The experimental test matrix is presented in Table 2. Here, Baseline test is the contrast condition where the pebble bed is entirely filled with



Fig. 6. Comparison of two sizes of alumina particles.

Table 2
Test matrix.

CaseID	SphereA0 mass, g	SphereA1 mass, g	Crush percentage, %	Diameter range, mm	Packing factor, %
Baseline	2633.9	0	0	1.0-1.2	0.613
CP3	2554.9	79.0	3	0.2-1.2	0.613
CP5	2502.2	131.7	5	0.2-1.2	0.613
CP7	2449.5	184.4	7	0.2-1.2	0.613
CP9	2396.8	237.1	9	0.2-1.2	0.613

large alumina particles. CP3 to CP9 correspond to situations with breakage rates of 3%, 5%, 7%, and 9%, respectively. In this study, the breakage rate represents the ratio of the mass of small particles to the total mass of the pebble bed.

$$\eta = M_{A1}/(M_{A0} + M_{A1}) \quad (1)$$

Where η represents the breakage rate, M_{A0} denotes the mass of large alumina particles in the pebble bed, and M_{A1} represents the mass of small aluminum oxide particles in the pebble bed. The experimental conditions for particle breakage were conducted based on the Baseline condition. By adjusting the masses of large and small particles under a certain total mass of the pebble bed, different breakage rates were obtained. Since the total mass of the pebble bed remains constant, the overall packing fraction of the pebble bed does not change with different breakage rates. In this paper, all test conditions are conducted at room temperature.

To accurately investigate the influence of helium gas velocity on pressure drop, this study did not use the pressure drop between random pairs of pressure guide tube or the pressure drop between a single guide tube and the inlet as the final experimental results. This is due to two considerations: (1) The need to eliminate the pressure drop caused by the filters. (2) The inlet and outlet sections of the pebble bed will disturb the helium gas flow field. Due to the reasons mentioned above, only four pressure differentials (dp_2 , dp_3 , dp_4 , dp_5) measured at points 2, 3, 4, and 5, respectively, were used. To mitigate errors resulting from individual measurements and non-uniform pebble bed packing and take advantage of the experimental data from the four measure points, the pebble bed pressure gradient $\Delta p/L$ was calculated as the average of the pressure drops across three different lengths, as shown in Eq. (2).

$$\frac{\Delta p}{L} = \frac{1}{3} \left(\frac{dp_5 - dp_2}{3l} + \frac{dp_4 - dp_2}{2l} + \frac{dp_3 - dp_2}{l} \right) \quad (2)$$

Where $\Delta p/L$ represents the pebble bed pressure gradient, in Pa/m.

dp_n represents the pressure differential measured between the inlet and the n th measure point. l represents the distance between adjacent pressure tapping points, which is 100 mm in this study.

3. Results and discussion

3.1. Comparison between baseline experiments and empirical equations

Firstly, the baseline experiment was carried out. Fig. 7 presents the pressure difference at different measurement points along the pebble bed under different flow velocities. The pebble bed lengths measured at points 1-6 increase sequentially. The longer the length, the greater the measured pressure drop. The pressure drop at these different positions increase with the increases in flow velocity and exhibit an approximate linear relationship.

For the study of characteristics in porous media flow, scholars have proposed numerous empirical correlations. In this study, we have selected three widely applicable correlations to compare with the pressure gradient obtained from the baseline experiments. These correlations include the Ergun equation [17], the Founmeny equation [18], and the Reichelt equation [19].

(1) Ergun equation:

$$\frac{\Delta p}{L} = C_1 \frac{(1 - \epsilon)^2}{\epsilon^3} \frac{\mu u}{d^2} + C_2 \frac{1 - \epsilon}{\epsilon^3} \frac{\rho u^2}{d} \quad (3)$$

Where, u represents the superficial velocity of the fluid, which is equivalent to the inlet velocity in this context, ϵ is the porosity of the pebble bed, μ represents the dynamic viscosity of the fluid, ρ is the fluid density, d stands for the diameter of the pebble bed particles, and C_1 and C_2 are constants where typically $C_1=150$ and $C_2=1.75$. The Ergun equation does not account for wall effects and is applicable when the ratio of the diameter of the pebble bed container D to the diameter of the pebbled satisfies $D/d \gg 10$. Additionally, the Ergun equation is applicable within the range of particle Reynolds numbers $0.4 \leq Re_{dp} \leq 1000$ where $Re_{dp} = \rho u d / \mu (1 - \epsilon)$.

(2) Founmeny equation:

$$\frac{\Delta p}{L} = 130 \frac{(1 - \epsilon)^2}{\epsilon^3} \frac{\mu u}{d^2} + \frac{D/d}{2.28 + 0.335(D/d)} \frac{1 - \epsilon}{\epsilon^3} \frac{\rho u^2}{d} \quad (4)$$

The Founmeny equation is applicable within the range of particle Reynolds numbers $5 \leq Re_{dp} \leq 8500$. Additionally, it demonstrates higher reliability when the diameter ratio within $3.23 < D/d < 23.8$.

(3) Reichelt equation:

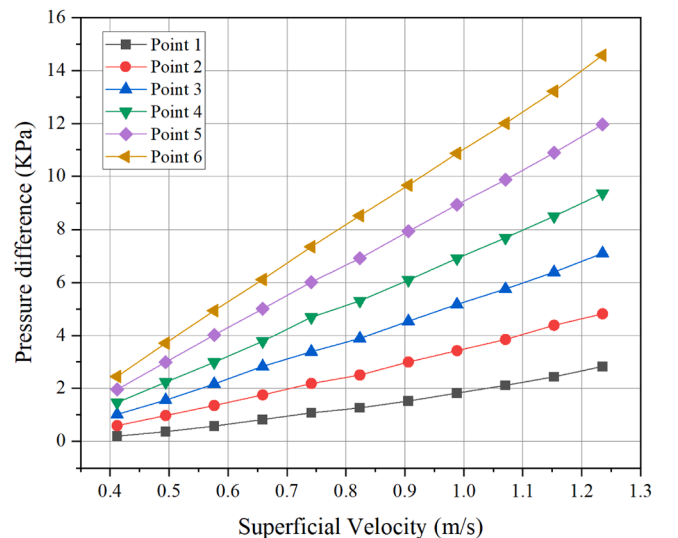


Fig. 7. Pressure difference at different positions in the baseline test.

$$\frac{\Delta p}{L} = K_1 \frac{(1-\varepsilon)^2}{\varepsilon^3} \frac{\mu u}{d^2} M^2 + \frac{(1-\varepsilon)}{\varepsilon^3} \frac{\rho u^2}{d} \frac{M}{B_w} \quad (5)$$

$$M = 1 + \frac{2}{3(D/d)(1-\varepsilon)} \quad (6)$$

$$B_w = (k_1(d/D) + k_2)^2 \quad (7)$$

In the Reichelt equation, two different terms denoted as M and B_w , are employed to describe wall effects at various Reynolds numbers. For cases where the diameter ratio $1.73 < D/d < 91$, $K_1=150$, $k_1=1.5$, $k_2=0.88$.

In our experiment, $D/d \geq 50$ and $3 \leq Re_{dp} \leq 15$, which satisfies the applicable ranges of the mentioned equations. The gas density and viscosity used in the equation are obtained through the average pressure within the pebble bed, which can be calculated by the data from absolute pressure gauges at the inlet and a series of pressure transmitters within the pebble bed. Fig. 8 illustrates the variations of the pebble bed pressure gradient with inlet velocity for the baseline experiment and the three empirical equations. At the range of inlet velocities from 0.4 m/s to 1.2 m/s, all three equations demonstrate a high level of agreement with the experimental data. The Founeney equation shows better consistency in a relatively low flow velocity, while the Reichelt equation is more effective in a higher flow velocity. The relative deviations between each equation and the experimental data are presented in Table 3. Among the three equations, the Reichelt equation exhibits the largest maximum relative deviation, at 17.49%. The Founeney equation shows the smallest maximum relative deviation and average absolute relative deviation, at 3.86% and 2.26% respectively. Overall, all three equations demonstrate a good ability to predict the pebble bed flow pressure drop within the experimental velocity range.

3.2. The effects of particle breakage rate on bed pressure drop

Fig. 9 illustrates the pressure drop across the pebble bed under different levels of particle breakage. It can be seen that the pressure drop increases with the increase in particle breakage rate, reaching its maximum at the highest particle breakage rate. In this experiment, the maximum designed particle breakage rate is 9%. At this level of breakage, the pressure drop in the pebble bed is approximately 1.6 times that of the baseline experiment. As the total mass of the pebble bed remains unchanged for different breakage rates, the macroscopic porosity of the pebble bed remains constant. However, the particle crushing pebble bed in this experiment is samiliar to the binary pebble

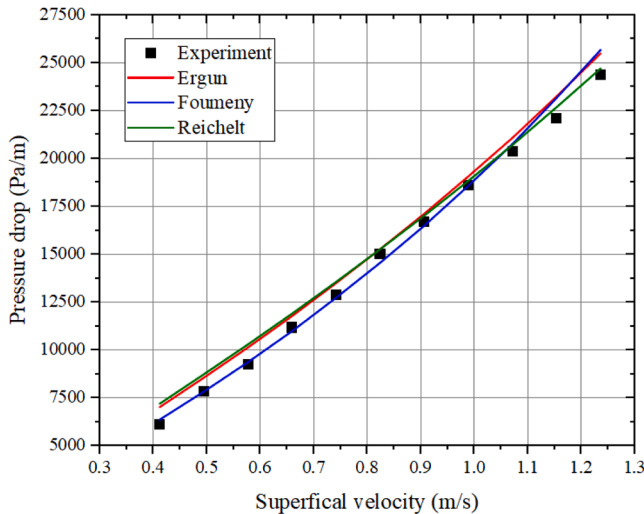


Fig. 8. Comparison between baseline experimental data and empirical equations.

Table 3

Pressure drop deviation between correlation and experiment.

Correlations	Maximum deviation, %	Mean absolute deviation, %
Ergun	14.56	5.75
Founeney	3.86	2.26
Reichelt	-17.49	5.66

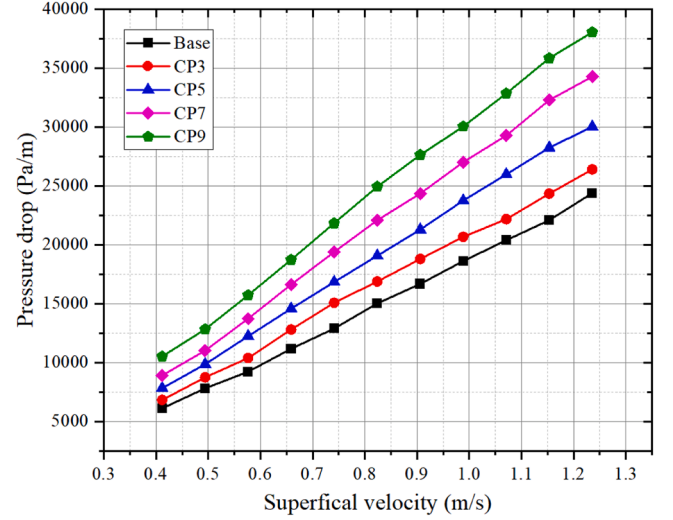


Fig. 9. Relationship between pressure drop and superficial velocity under different breakage rates.

bed, and the latter tend to have a higher packing factor. Therefore, the increase in pressure drop may be attributed to the decrease in local porosity and the reduction in average particle size.

In order to characterize the influence of particle breakage phenomena on the pressure drop across the pebble bed, we modified the constant of Ergun equation C_1 and C_2 to meet the prediction of experiment result. The adjusted coefficients are presented in Table 4. For the baseline case, the value of C_2 is reduced to 1.5, resulting in a better fit at high flow rates. Fig. 10 illustrates the comparison between the modified Ergun equation and the experimental data. The maximum and average relative deviation between the adjusted values and the experimental results are both within 5%, indicating a good agreement.

3.3. The flow pressure drop model of particle-crushed pebble bed

To facilitate the estimation of helium flow pressure drop within the range of 3% to 9% particle breakage rates, the Ergun equation coefficients under different breakage rates from Table 4 were connected with the particle breakage rate η . The fitted curve are shown in Fig. 11, where (a) represents a quadratic polynomial fitting for the coefficient C_1 , with an R-squared value of 0.997, and (b) represents a linear fitting for the coefficient C_2 , with an R-squared value of 0.919. The fitted coefficients are C_1^* and C_2^* as shown in Eqs. (8) and (9). Although the linear fitting deviation for C_2 seemsless accurate, since the second term of the Ergun equation is mainly used to describe the flow pressure drop

Table 4

Corrected coefficients of the Ergun correlation with different breakage rate.

Breakage rate (%)	C_1	C_2
0	150	1.50
3	159.52	1.75
5	178.09	2.49
7	197.18	2.65
9	232.20	2.79

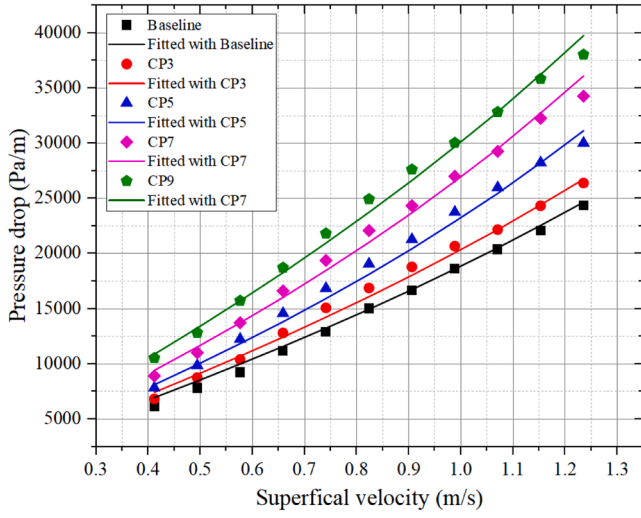


Fig. 10. Comparison of experimental result with fitted Ergun equation.

dominated by inertial force, for the helium-cooled solid breeder bed with a low design flow rate, this term does not have a significant impact on the overall pressure drop, this deviation is acceptable.

$$C_1^* = 150 + 35\eta + 9616\eta^2 \quad (8)$$

$$C_2^* = 15.77\eta + 1.48 \quad (9)$$

$$\frac{\Delta p}{L} = C_1^* \frac{(1 - \varepsilon)^2}{\varepsilon^3} \frac{\mu u}{d^2} + C_2^* \frac{1 - \varepsilon}{\varepsilon^3} \frac{\rho u^2}{d} \quad (10)$$

The established model for pebble bed pressure drop applicable to particle breakage rates of 3% to 9%, as shown in Eq. (10), where C_1^* and C_2^* are functions of the particle breakage rate η . Fig. 12 illustrates the flow pressure drop predicted by the empirical correlation for intact pebble bed and pebble bed with breakage rates of 3%, 5%, 7%, and 9%, with a maximum relative deviation of 13.4%. This indicates that the empirical formula can accurately predict the flow pressure drop within this range. In practice, achieving a particle breakage rate of 9% or higher is quite impossible. Therefore, the empirical formula can effectively predict the flow pressure drop in the particle crushing helium-cooled solid breeder bed with particle diameters about 1 mm.

4. Conclusions

The helium flow pressure drop experiment in the intact pebble bed (alumina, diameter 1.0–1.2 mm) and the particle crushing pebble bed (alumina, breakage rate 3%, 5%, 7%, 9%) were carried out by the pebble bed pressure test facility. The effects of different flow rates and breakage rates on the pressure drop were investigated. For all experimental pebble beds, the pressure drop increased with increasing flow rate. The pressure drop data from the single-diameter pebble bed experiments were compared with three different empirical relationships, including the Ergun equation, Fomenko equation, and Reichelt equation. All three equations effectively predicted the pressure drop within the experimental design flow rate range. In the case of broken pebble beds, the pressure drop increased with increasing breakage rate. At a breakage rate of 9%, the pebble bed flow pressure drop increased by approximately 1.6 times. By modifying the two constants, C_1 and C_2 of the Ergun equation, the flow pressure drops of pebble beds with different particle breakage rates were accurately predicted. By fitting of the modified constant coefficients of the Ergun equation, we established a correlation suitable for particle crushing pebble beds. The study of helium flow pressure drop in particle crushing pebble beds provided relevant experimental data, offering valuable insights for the reliable design of future helium-cooled ceramic breeding bed.

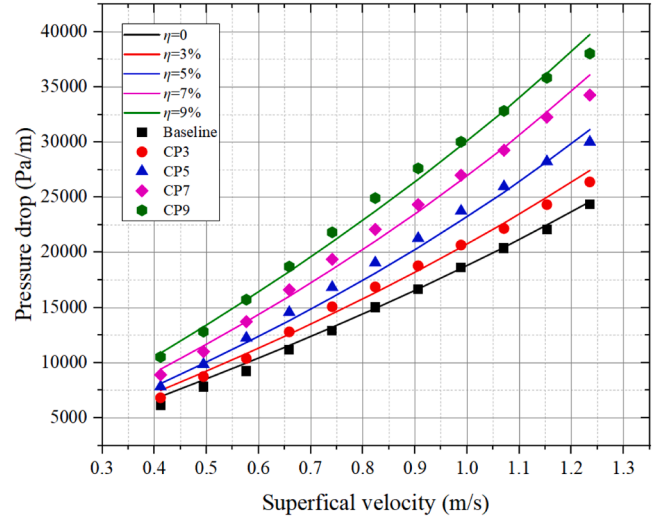


Fig. 12. Comparison of experimental result with fitted equation.

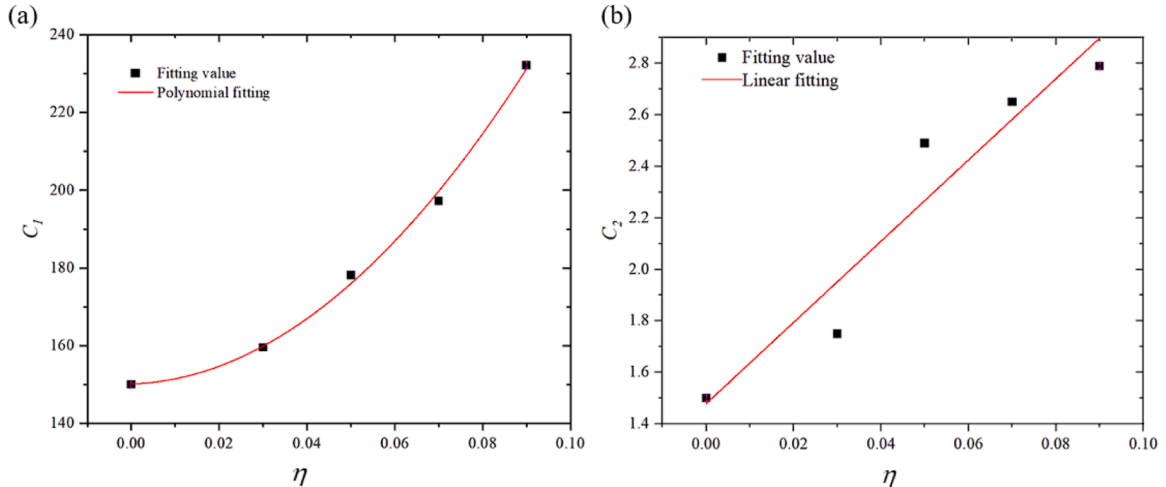


Fig. 11. Polynomial fitting with the fitted Ergun constant term, (a) C_1 , (b) C_2 .

CRediT authorship contribution statement

Hao Cheng: Writing – review & editing, Writing – original draft, Visualization, Methodology, Investigation, Formal analysis, Conceptualization. **Zheng Fang:** Writing – review & editing, Writing – original draft, Methodology, Investigation, Formal analysis, Data curation, Conceptualization. **Bing Zhou:** Writing – review & editing, Resources, Project administration, Conceptualization. **Baoping Gong:** Writing – review & editing, Supervision, Project administration, Methodology, Conceptualization. **Shanshan Bu:** Writing – review & editing, Supervision, Methodology, Investigation, Funding acquisition, Conceptualization. **Zhenzhong Li:** Writing – review & editing, Supervision, Methodology, Conceptualization. **Deqi Chen:** Writing – review & editing, Supervision, Methodology, Conceptualization.

Declaration of competing interest

The authors declare that they have no known competing financial interests or personal relationships that could have appeared to influence the work reported in this paper.

Data availability

Data will be made available on request.

Acknowledgments

We would like to acknowledge financial supports for this work provided by the National Natural Science Foundation of China (No. 52276052) and the Natural Science Foundation of Sichuan, China, (Grant No. 2022NSFSC1216).

References

- [1] Luciano M. Giancarli, Xavier Bravo, Seungyon Cho, et al., Overview of recent ITER TBM Program activities, *Fusion Eng. Des.* (2020) 158.
- [2] Yuanxi Wan, Jiangang Li, Yong Liu, et al., Overview of the present progress and activities on the CFETR, *Nucl. Fusion* 57 (10) (2017).
- [3] Ali Abou-Sena, Frederik Arbeiter, Lorenzo V. Boccaccini, et al., Experimental study and analysis of the purge gas pressure drop across the pebble beds for the fusion HCPB blanket, *Fusion Eng. Des.* 88 (4) (2013) 243–247.
- [4] Ali Abou-Sena, Frederik Arbeiter, Lorenzo V. Boccaccini, et al., Measurements of the purge helium pressure drop across pebble beds packed with lithium orthosilicate and glass pebbles, *Fusion Eng. Des.* 89 (7–8) (2014) 1459–1463.
- [5] Mingjun Wang, Di Liu, Yan Xiang, et al., Experimental study of the helium flow characteristics in pebble-bed under the condition of CFETR's blanket module, *Progr. Nucl. Energy* 100 (2017) 283–291.
- [6] Di Liu, Wenxi Tian, G.H. Su, et al., Experimental study on helium pressure drop across randomly packed bed for fusion blanket, *Fusion Eng. Des.* 122 (2017) 47–51.
- [7] Maulik Panchal, Abhishek Saraswat, Paritosh Chaudhuri, Experimental measurements of gas pressure drop of packed pebble beds, *Fus. Eng. Des.* (2020) 160.
- [8] Yong Liu, Yong Chen, Cong Wang, et al., Measurement of pressure drop of purge gas flow in unitary and binary pebble beds, *Fusion Eng. Des.* (2024) 203.
- [9] G. Piazza, A. Erbe, R. Rolli, et al., Post-irradiation examinations of Li₄SiO₄ pebbles irradiated in the EXOTIC-8 experiment, *J. Nucl. Mater.* 329–333 (2004) 1260–1265.
- [10] S. Van Til, A.V. Fedorov, A.J. Magielsen, Study of ceramic pebble beds in Post Irradiation Examination of the Pebble Bed Assemblies irradiation experiment, *Fusion Eng. Des.* 87 (5–6) (2012) 885–889.
- [11] G. Dell'orco, A. Ancona, A. Dimaio, et al., Thermo-mechanical testing of Li–ceramic for the helium cooled pebble bed (HCPB) breeding blanket, *J. Nucl. Mater.* 329–333 (2004) 1305–1308.
- [12] Shuo Zhao, Yixiang Gan, Marc Kamlah, et al., Influence of plate material on the contact strength of Li₄SiO₄ pebbles in crush tests and evaluation of the contact strength in pebble–pebble contact, *Eng. Fracture Mech.*, 100 (2013) 28–37.
- [13] Raghuram Karthik Desu, Paritosh Chaudhuri, Ratna Kumar Annabattula, High temperature oedometric compression of Li₂TiO₃ pebble beds for Indian TBM, *Fusion Eng. Des.* 136 (2018) 945–949.
- [14] R.K. Annabattula, M. Kolb, Y. Gan, et al., Size-dependent crush analysis of lithium orthosilicate pebbles, *Fusion Sci. Technol.* 66 (1) (2014) 136–141.
- [15] Mingzhun Lei, Qigang Wu, Shuling Xu, et al., Crushing behaviour of Li₄SiO₄ and Li₂TiO₃ ceramic particles, *Nucl. Mater. Energy* (2022) 31.
- [16] Jian Wang, Mingzhun Lei, Hao Yang, et al., Predicting the crushing behavior of pebbles: theoretical model and experiment verification, *Fusion Eng. Des.* (2023) 194.
- [17] Sabri Ergun, Ao Ao Orning, Fluid flow through randomly packed columns and fluidized beds, *Ind. Eng. Chem.* 41 (6) (1949) 1179–1184.
- [18] E.A. Foumeny, F. Benyahia, J.A.A. Castro, et al., Correlations of pressure drop in packed beds taking into account the effect of confining wall, *Int. J. Heat. Mass Transf.* 36 (2) (1993) 536–540.
- [19] Wolfgang Reichelt, Zur Berechnung des Druckverlustes einphasig durchströmter Kugel- und Zylinderschüttungen, *Chemie Ingenieur Technik - CIT* 44 (18) (1972) 1068–1071.